Analysis of the ionic current in a *Loligo* axon during a voltage clamp. Trace *a* shows the response to a depolarization of 56 mV with the axon in sea water. Trace *b* is the response with the axon in a solution comprising

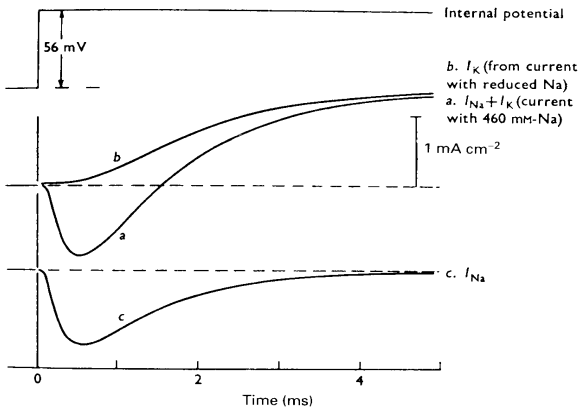

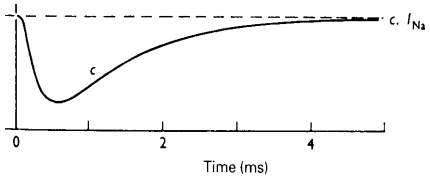

From traces of Na current as a function of time we can obtain g_{Na} by using the equation $I_{Na}=g_{Na}(E-E_{Na})$. E_{Na} is the potential at which the current is nulled.

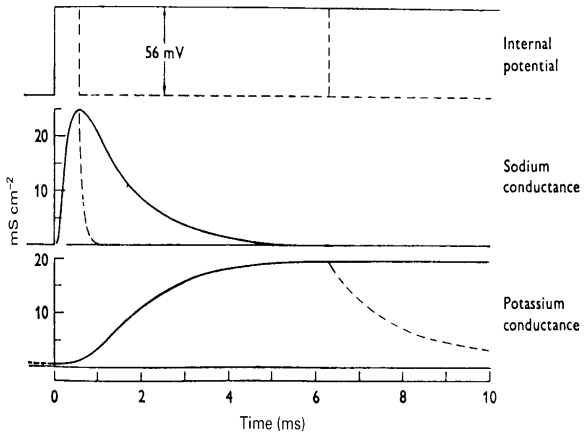

Ionic conductance changes during a clamped depolarization, derived from the current curves shown in fig. 5.12. The broken curves show the effects of repolarization. (From Hodgkin, 1958, by permission of the Royal Society.)

If we knew the time and voltage dependence of gNa and gK we could obtain the form the the action potential by numerical integration of the following equation.

$$I_m = C_m dV/dt + g_k(E-E_k) + g_{Na}(E-E_{Na}) + g_l(E-E_l)$$

Conductance changes brought about by clamped depolarizations of different extents. The circles represent values derived from the experimental measurements of ionic current, and the curves are drawn according to the equations used to describe the conductance changes. (From Hodgkin, 1958, after Hodgkin and Huxley, 1952*d*.)

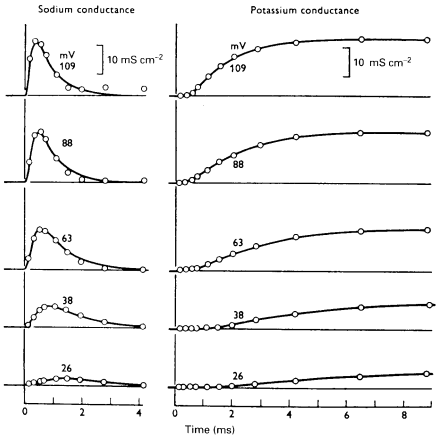

$g_K = \bar{g}_K\, n^4$ n=probability of 4 charged particles being in the correct configuration for conduction.

$g_{Na} = \bar{g}_{Na}\, m^3h$ n=probability of 3 charged particles being in the correct configuration.1-h=probability of inactivation.

n is the potassium activation parameter,m and h are the Na activation and inactivation parameters.

$I_m = C_m dE/dt + I_k + I_{Na} + I_i$

$= C_m dV/dt + g_k(E-E_k) + g_{Na}(E-E_{Na}) + g_l(E-E_l)$

$= C_m dV/dt + \bar{g}_{Na} n^4(E-E_k) + \bar{g}_{Na} m^3h\,(E-E_{Na}) + g_l(E-E_l)$

With the voltage and time dependence of m,n and h the above equation can be solved for V by numerical integration

Calculated changes in membrane potential (upper curve) and sodium and potassium conductances (lower curves) during a propagated action potential in a squid giant axon. The scale of the vertical axis is correct, but its position may be slightly inaccurate; it has been drawn here assuming a resting potential of −60 mV. The positions of E_{Na} and E_K are correct with respect to the resting potential. In the original calculations, voltages were measured from the resting potential, as in fig. 5.15. (After Hodgkin and Huxley, 1952*d*; redrawn.)

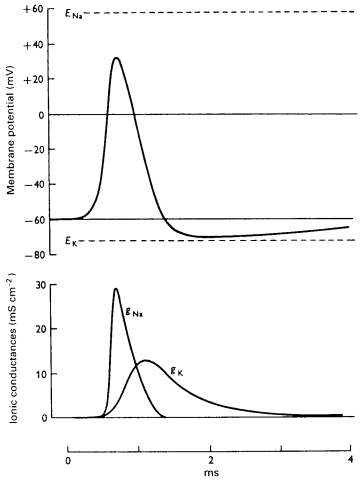

Comparison of computed (*a*) and observed (*b*) propagated action potentials in squid axon at 18.5 °C. The calculated velocity of conduction was 18.8 m s^{-1}; the observed velocity was 21.2 m s^{-1}. (From Hodgkin and Huxley, 1952*d*.)

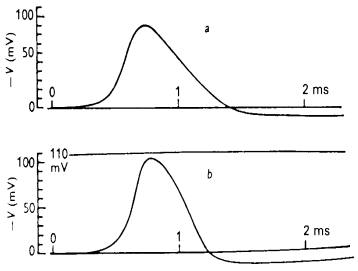

Voltage-clamp records for frog nodes, showing separation of the sodium and potassium currents by the use of selective blocking agents. The membrane potential was clamped at −120 mV for 40 ms before the start of the records, and then depolarised to various levels ranging from −60 to +60 mV in 15 mV steps. Leakage and capacity currents were subtracted by computer. Records in *a* and *c* show the normal response. In *b* the node shown in *a* was treated with 300 nM tetrodotoxin; only the potassium current remains. In *d* the node shown in *c* was treated with 6 mM TEA; only the sodium current remains. (From Hille, 1984, after Hille, 1966 and 1967.)

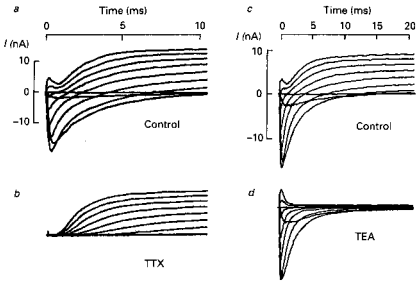

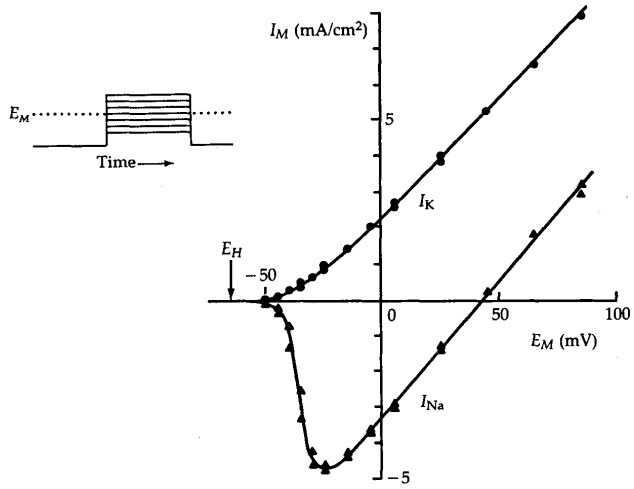

A sketch to show the main features of the sodium channel. (Based partly on diagrams by Armstrong, 1981, and Hille, 1984.)

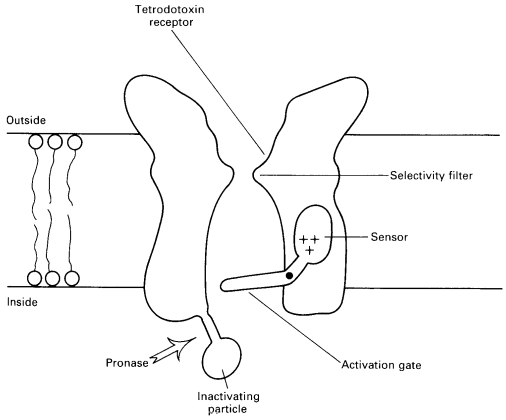

Sodium ionic and gating currents in squid axon, produced during depolarizations under voltage clamp. The upper traces show currents recorded in an artificial sea water with only one fifth of the normal sodium concentration, for depolarizations from −70 mV to −20, 0 and +20 mV. The initial brief outward current is gating current, followed by the much larger inward sodium ionic current. The lower set shows the gating currents alone, after blockage of the sodium ionic currents with tetrodotoxin. Potassium currents were eliminated by using potassium-free solutions for both internal and external media. (From Bezanilla, 1986.)

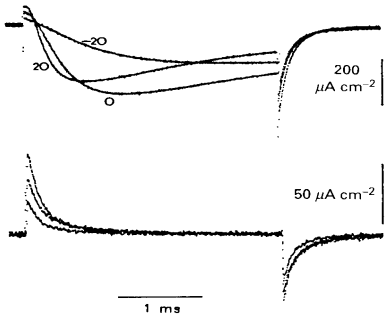

Schematic diagram showing one way in which gating currents could arise. The capacity currents are much larger than the gating currents.

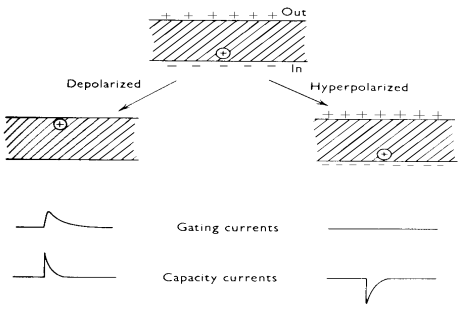

Patch-clamp recording. The polished end of a microelectrode is pushed against the cell surface and suction is applied to the electroyte in it. This produces a high-resistance seal between the edge of the electrode and the membrane, and the preparation is then ready for cell-attached recording (*a*). Various further treatments, also shown in *a*, allow access to the whole cell or to the inner or outer surfaces of separated patches of membrane. The voltage-clamp circuit (*b*) consists of a high-gain amplifier (FBA) in which the output (on the right) is fed back via the resistor *R* to the input. This ensures that the input voltage *V* is kept very nearly equal to the signal voltage *V*. The output is proportional to the current flowing through the patch of membrane in contact with the electrode. (*a* from Hamill et al., 1981.)

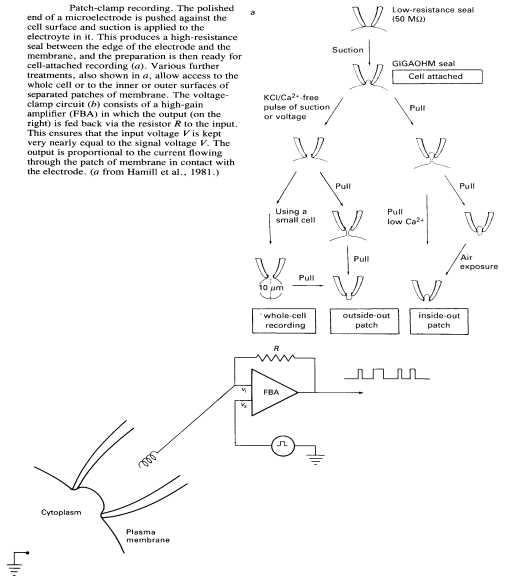

Single sodium channel currents from cultured rat muscle cells, recorded with the cell-attached patch-clamp technique. Trace *a* shows the imposed membrane potential, held at $V = -30$ mV (where V = 0 is the resting potential) and depolarized by 40 mV to $V = +10$ mV for about 23 ms at 1 s intervals. Trace *b* shows the average of a set of 300 of current records elicited by these pulses. *c* shows nine successive individual records from this set. Square pulses of inward current (average size 1.6 pA) can be seen in most of the records; these correspond to the opening of individual channels. Trace *d* shows a record taken when two thirds of the sodium ions in the pipette had been replaced with tetramethylammonium ions; the single-channel current is reduced accordingly. (From Sigworth and Neher, 1980.)

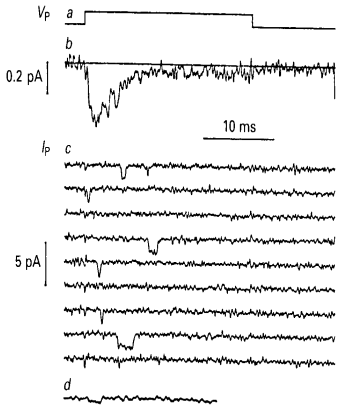

Channel (Gating) Simulations

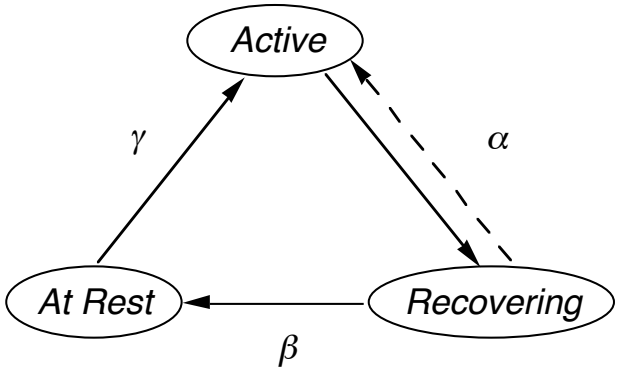

α, β, γ: state transition probabilities, (functions of v and t)

Action Potential from Different Cells

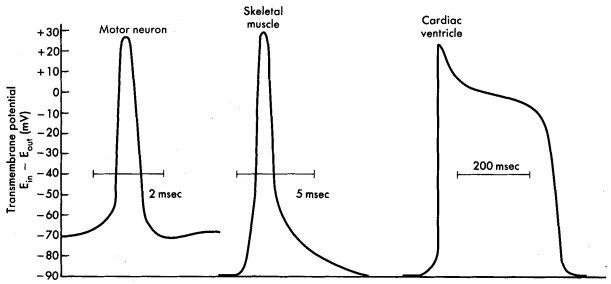

Action potentials from three vertebrate cell types. Note the different time scales.
(Redrawn from Flickinger CJ et al: *Medical cell biology,* Philadelphia, 1979, WB Saunders.)

Cardiac Action Potential

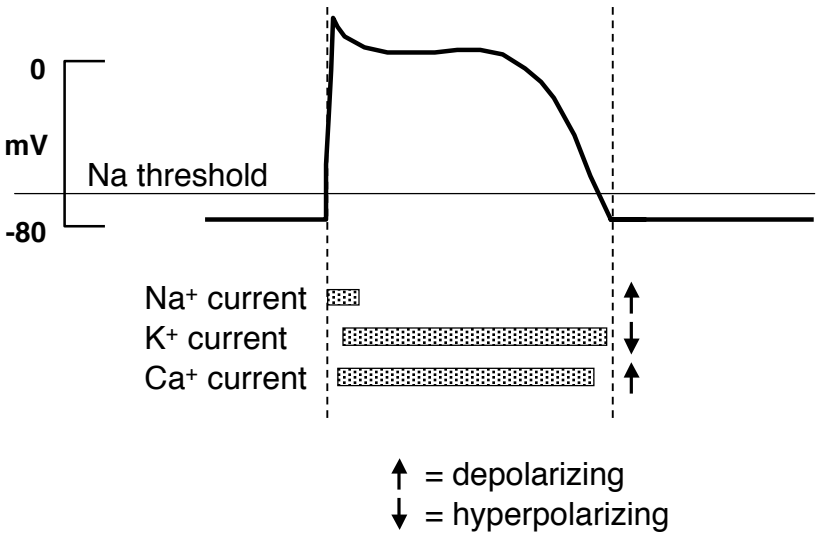

Cardiac Cell Currents

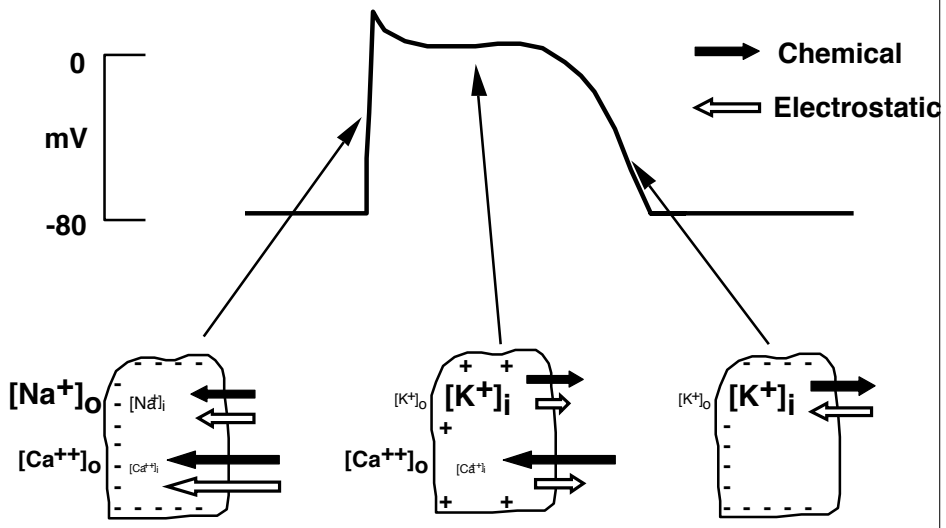

Cardiac Ion Currents

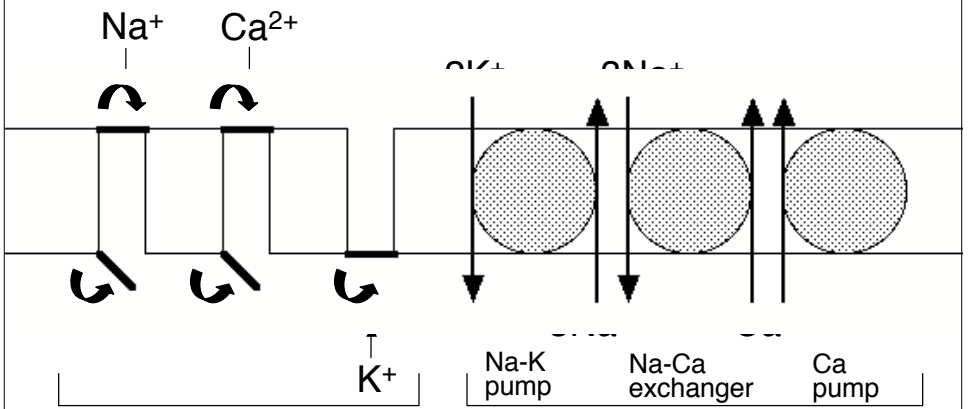

Ion channels

- Passive ion movement
- Driven by concentration and electrostatic gradients
- Channels are selective
- Gates control opening

Carrier mediated ion transport

- Na-K and Ca pumps require ATP
- Capable of driving against concentration gradient
- Na-Ca exchange does not require ATP

Calcium Cycle in Cardiac Muscle

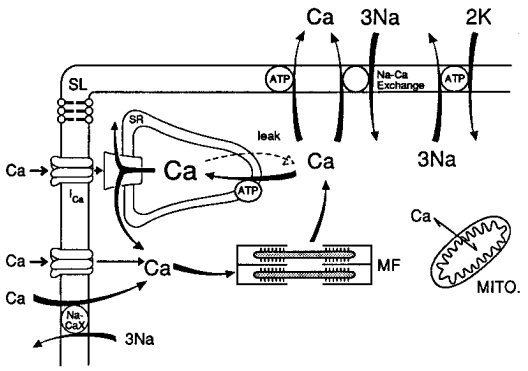

General scheme of Ca cycle in a cardiac myocyte. Ca can enter via Ca channels and Na/Ca exchange. Ca current may also control the SR Ca release by the SR Ca release channel/ ryanodine receptor/ foot protein. Ca is removed from the myofilaments (MF) and cytoplasm by the SR Ca-ATPase pump and the sarcolemmal Ca-ATPase pump and Na/Ca exchange.

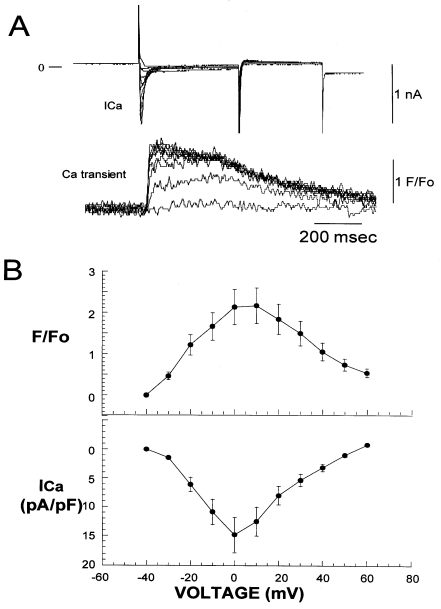

Calcium Transients.